



Fabrication and corrosion behavior of Ti-based bulk metallic glass composites containing carbon nanotubes

Chih-Feng Hsu^a, Wu Kai^a, Hong-Ming Lin^b, Chung-Kwei Lin^c, Pee-Yew Lee^{a,*}

^a Institute of Materials Engineering, National Taiwan Ocean University, 2, Pei-Ning Road, Keelung, Taiwan

^b Department of Materials Engineering, Tatung University, Taipei, Taiwan

^c Department of Materials Science and Engineering, Feng Chia University, Taichung, Taiwan

ARTICLE INFO

Article history:

Received 2 July 2009

Received in revised form 18 January 2010

Accepted 10 February 2010

Available online 18 February 2010

Keywords:

Mechanical alloying

Bulk metallic glass composite

Supercooled liquid region

Vacuum hot pressing

Corrosion resistance

ABSTRACT

This study explored the feasibility of preparing Ti₅₀Cu₂₈Ni₁₅Sn₇ bulk metallic glass composite with powder metallurgy. With high energy ball milling of a pure Ti, Cu, Ni, Sn and carbon nanotube (CNT) powder mixture, the CNT/Ti₅₀Cu₂₈Ni₁₅Sn₇ metallic glass composite powders can be formed with mechanical alloying (MA) after 8 h milling. The bulk metallic glass composite was successfully prepared by vacuum hot pressing the as-milled CNT/Ti₅₀Cu₂₈Ni₁₅Sn₇ metallic glass composite powders. The corrosion behavior of the Ti₅₀Cu₂₈Ni₁₅Sn₇ bulk metallic glass as well as composites modified by the addition of CNT was investigated by electrochemical measurements. Electrochemical characterization was performed in Hanks' solution at 37 °C with physiologically relevant dissolved oxygen content. The results of potentiodynamic polarization measurements revealed that the Ti-based bulk metallic glass composites examined showed spontaneous passivity by anodic polarization with a passive current density of about 10⁻⁵ A/cm². The higher corrosion resistance of the Ti-based bulk metallic glass composites was attributed to stable and protective passive films enriched with titanium containing certain amounts of additional elements.

© 2010 Elsevier B.V. All rights reserved.

1. Introduction

Bulk metallic glasses (BMGs) have attracted much attention due to their unique properties, for example, superior strength, high hardness, excellent corrosion resistance and high wear resistance [1]. For application of metallic glasses alloys to engineering fields, it is important to characterize their corrosion characteristics due to the requirement of high chemical stability in service environments. Ti-based bulk metallic glasses were first reported in the Ti–Zr–Ni–Be system in 1994 [2]. To improve the mechanical properties or corrosion characteristics of such single-phase metallic glasses alloys, metallic glass matrix composites were developed. The glasses were reinforced by second-phase particulates [3], fibers [4], or in situ formed ductile phase precipitates [5]. Recently, many techniques have been used successfully to prepare Ti-based BMGs, but most research efforts and industrial interest are focused on the different implementations of the rapid solidification [6]. An alternative method is using a solid-state amorphization processing, for instance, mechanical alloying (MA), to prepare amorphous powders that are suitable for further compaction and densification. Meanwhile, reinforced particles can be introduced easily into the

glassy matrix. As previous investigations have demonstrated, MA has been used successfully to prepare amorphous Cu- and Zr-based composite powders [7,8].

Even though BMGs and CNTs have many excellent properties, a literature survey indicated no report on the formation of Ti-based BMG composite powder containing CNTs by the MA process. By adding CNTs into Ti-based BMGs, performance improvements can be anticipated. In contrast to several investigations reported on corrosion studies on Zr-based amorphous alloys [9], only a few investigations on Ti-based amorphous alloys exist [10]. In this work, amorphous Ti₅₀Cu₂₈Ni₁₅Sn₇ powders with or without CNT were prepared by MA. Subsequent consolidation of as-milled powders was performed, and the corrosion resistances in simulated body fluid of Ti₅₀Cu₂₈Ni₁₅Sn₇ BMG composites were investigated.

2. Experimental procedure

A mixture of elemental metallic powders with a nominal composition of Ti₅₀Cu₂₈Ni₁₅Sn₇ (in at.%) was mechanically alloyed with or without the addition of 4, 8 and 12 vol.% CNT powders. The milling was performed in a SPEX 8016 shaker ball mill under an Ar-filled atmosphere. Specific details of the mechanical alloying process are described elsewhere [7]. The as-milled composite powders were consolidated in a vacuum hot pressing machine to prepare bulk samples with a 10 mm diameter and 2 mm thickness. The structures of the as-milled and bulk samples were analyzed using an X-ray diffractometer and scanning electron microscope. Thermal analysis was investigated using a Dupont 2000 differential scanning calorimeter (DSC), in which the sample was heated from room temperature to 900 K under a purified argon atmosphere at a constant heating rate of 40 K/min. In addition,

* Corresponding author.

E-mail address: pylee@mail.ntou.edu.tw (P.-Y. Lee).

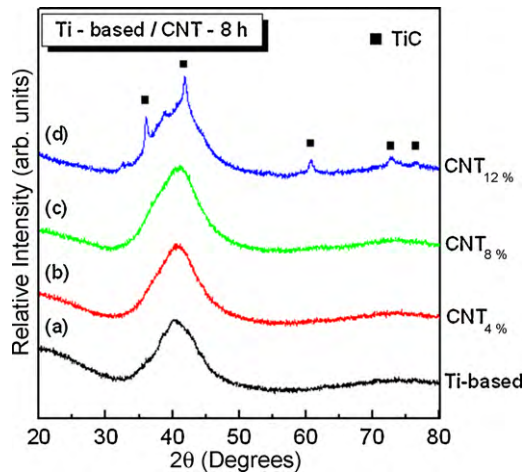


Fig. 1. X-ray diffraction patterns for mechanically alloyed $\text{Ti}_{50}\text{Cu}_{28}\text{Ni}_{15}\text{Sn}_7$ and composite powders after 8 h milling.

the corrosion behavior of the bulk glassy alloys was evaluated by electrochemical measurements. For each condition, at least three samples were examined and the middle data was presented. Prior to corrosion testing, the samples were mechanically polished with silicon carbide papers up to grit 2000. The electrolyte used was simulated body fluid Hanks' solution with pH 7.4 at 310 K open to air, which was prepared from reagent grade chemicals and deionized water. The composition of Hanks' solution (g/L) is 8.00 NaCl, 0.40 KCl, 0.35 NaHCO_3 , 0.19 $\text{CaCl}_2 \cdot 2\text{H}_2\text{O}$, 0.09 $\text{Na}_2\text{HPO}_4 \cdot 7\text{H}_2\text{O}$, 0.2 $\text{MgSO}_4 \cdot 7\text{H}_2\text{O}$, 0.06 KH_2PO_4 , 1.00 glucose. Electrochemical measurements were conducted in a three-electrode cell using a platinum counter electrode and a saturated calomel reference electrode (SCE). Potentiodynamic polarization curves were measured with a potential sweep rate of 1.0×10^{-3} V/s in Hanks' solution after immersing the specimens for 1800 s, when the open-circuit potentials became almost steady. X-ray photoelectron spectroscopy (XPS) was performed on the surface of the bulk glassy alloys after immersion in Hanks' solution at 37 °C.

3. Results and discussion

The XRD patterns of the elemental powder mixture with a composition $\text{Ti}_{50}\text{Cu}_{28}\text{Ni}_{15}\text{Sn}_7$ after milling for 8 h are shown in Fig. 1(a). There is one clear broad diffraction peak around $2\theta = 42^\circ$, which indicates that fully amorphous powders were formed. As for the composite powders of $\text{Ti}_{50}\text{Cu}_{28}\text{Ni}_{15}\text{Sn}_7$ alloy mixed with 4 and 8 vol.% CNT after 8 h of milling, as seen in Fig. 1(b) and (c), no diffraction peaks from the crystalline CNT can be detected. This may be attributed to the small volume and crystalline size of CNT particles. Lin et al. [11] reported that for an addition of a small amount of Al_2O_3 to mechanically alloyed Ni–Al alloys no Al_2O_3 phase can be detected by XRD after 10 h milling. This is similar to what was observed in this work for the preparation of the NiAl– Al_2O_3 intermetallic–matrix composite. The XRD spectra of the 12 vol.% CNT-containing powders are also depicted in Fig. 1(d). The 12 vol.% CNT-containing powders exhibit a broad halo peak and sharp diffraction peaks superimposed, identified as TiC, which suggests the presence of a mixture of the amorphous and TiC crystalline phases.

In order to observe the microstructure within the bulk metallic glasses, $\text{Ti}_{50}\text{Cu}_{28}\text{Ni}_{15}\text{Sn}_7$ and its composite with 12 vol.% CNT additions, i.e., the same sample shown in Fig. 1, were examined by transmission electron microscopy. The TEM micrographs of $\text{Ti}_{50}\text{Cu}_{28}\text{Ni}_{15}\text{Sn}_7$ powder are shown in Fig. 2(a); a typical “salt and pepper” microstructure representing a homogeneous amorphous phase was observed. For a composite powder with 12 vol.% CNT, as revealed by TEM in Fig. 2(b), TiC nanoparticles with irregular shapes and sizes around 20–40 nm are embedded and homogeneously distributed in the amorphous matrix. The illustration included in Fig. 2(b) presents the selected area diffraction (SAD) pattern taken from the matrix, where a typical diffuse halo can be observed,

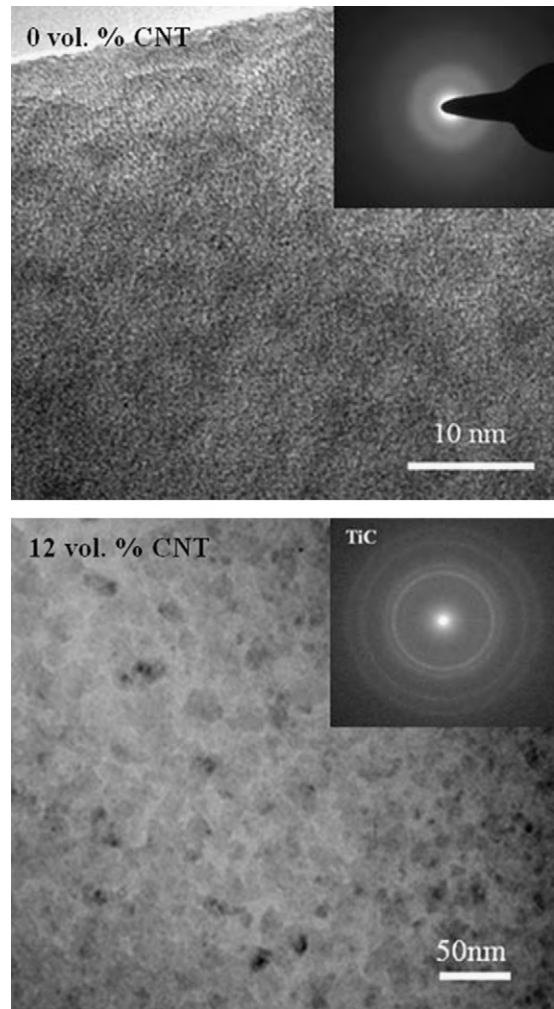


Fig. 2. TEM images of mechanically alloyed $\text{Ti}_{50}\text{Cu}_{28}\text{Ni}_{15}\text{Sn}_7$ and composite powders after 8 h of milling.

with the ring patterns of crystalline TiC representing the amorphous phase. This proves that the introduction of carbon induces the in situ formation of TiC particles, and the Ti-based multicomponent matrix remains amorphous due to its high glass-forming ability. According to the Miedema model [12], the mixing enthalpy (kJ/mol) calculated for Ti–C is -92 ; for Ti–Cu it is -9.6 , and for Ti–Ni it is -34 . This means that Ti has a greater chance than Cu, Ni and Sn metal to interact with C during the course of the in situ reaction, which leads to the precipitation of TiC particles over the amorphous matrix. A similar behavior has been reported by Bian et al. [13], who found that CNT can react with Zr and result in the formation of ZrC phase during the preparation of CNT reinforced Zr–Cu–Ni–Al–Ti bulk metallic glass composites by the conventional die cast method.

To investigate the glass transition and crystallization behavior of the as-milled powders, we used differential scanning calorimetry to scan the 8 h as-milled $\text{Ti}_{50}\text{Cu}_{28}\text{Ni}_{15}\text{Sn}_7$ monolithic glass and the composites with CNT particles, as shown in Fig. 3. The glass transition (T_g) and crystallization (T_x) temperatures are defined as the onset temperature of the endothermic and exothermic DSC events, respectively. The $\text{Ti}_{50}\text{Cu}_{28}\text{Ni}_{15}\text{Sn}_7$ without CNT particles exhibits T_g at 719 K and T_x at 765 K. The T_g and T_x of the composite powders are higher than those of the single-phase amorphous $\text{Ti}_{50}\text{Cu}_{28}\text{Ni}_{15}\text{Sn}_7$ alloy. The area of the crystallization peak also decreases dramatically when the CNT content exceeds 8%. In other words, from the results of XRD and TEM, as shown in Figs. 1 and 2, it appears that

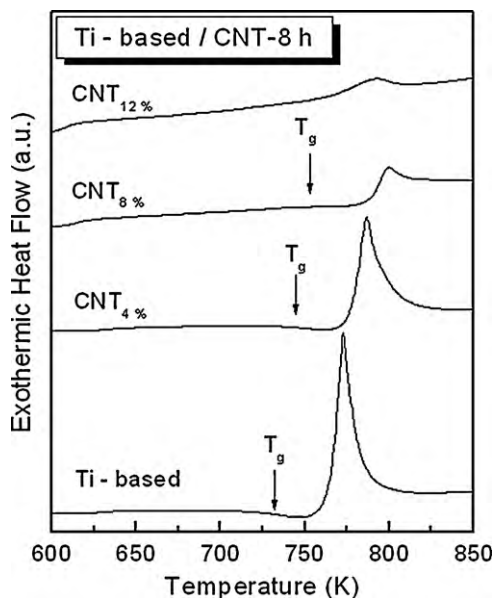


Fig. 3. DSC scans of mechanically alloyed $\text{Ti}_{50}\text{Cu}_{28}\text{Ni}_{15}\text{Sn}_7$ and composite powders after 8 h milling.



Fig. 4. The outer morphology of the $\text{Ti}_{50}\text{Cu}_{28}\text{Ni}_{15}\text{Sn}_7$ with 4 vol.% CNT addition after vacuum hot pressing at 723 K under a pressure of 1.2 GPa.

the in situ TiC phase formed during milling will induce the overall composition of the glassy phase to deviate from the starting composition and will finally change the thermal stability of the composite powders. Similar behavior was reported for small ZrC additions in a Zr–Al–Cu–Ni alloy by mechanical alloying [14]. Based on the DSC results, the 8 h as-milled composite powders were consolidated by vacuum hot pressing into a disk with a 10 mm diameter and 2 mm thickness. The powders were hot pressed at 723 K under a pressure of 1.2 GPa for 30 min. Fig. 4 shows a consolidated sample of the bulk metallic glass composite that exhibited a smooth outer surface and metallic luster. Though not shown here, consolidated BMG

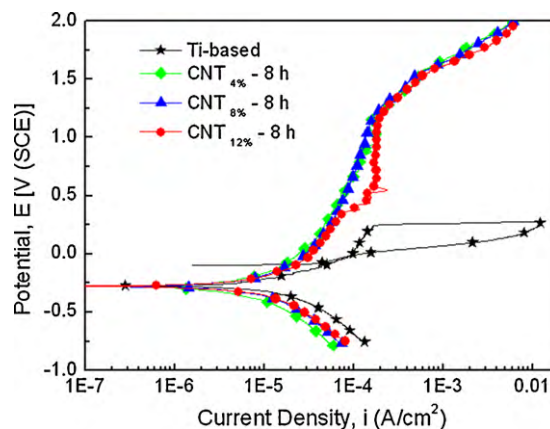


Fig. 5. Anodic and cathodic polarization curves of the $\text{Ti}_{50}\text{Cu}_{28}\text{Ni}_{15}\text{Sn}_7$ bulk metallic glasses containing CNT mixed 8 h in Hanks' solution at 310 K.

$\text{Ti}_{50}\text{Cu}_{28}\text{Ni}_{15}\text{Sn}_7$ and composite samples exhibited similar XRD and TEM results as those of the corresponding powders shown in Fig. 1 (XRD) and Fig. 2 (TEM).

Potentiodynamic polarization processing of Ti-based bulk metallic glasses revealed pitting corrosion. The corrosion potential and pitting potential are -273.5 mV and 249.1 mV (as listed in Table 1), respectively. However, the Ti-based bulk metallic glass composites containing 4%, 8% and 12% CNT did not exhibit pitting corrosion, and all potentiodynamic polarization curves were the same. Under high potential, the corrosion reaction of metal and H_2O electrolysis occurs, and the induced corrosion current density increases. Fig. 5 shows the potentiodynamic polarization that improves the corrosion resistance of Ti-based bulk metallic glass composites containing CNT. Morrison et al. [15] reported that the potentiodynamic polarization curves of $\text{Ti}_{43.5}\text{Zr}_{21.7}\text{Ni}_{7.5}\text{Be}_{27.5}$ BMG immersed in phosphate-buffered saline (PBS) solution showed pitting corrosion, and the measure values are -372 mV (E_{corr}) and 217 mV (E_{pit}). Qin et al. [10] observed that the corrosion resistance is improved when the Cu content decreases with an increase of Zr for $\text{Ti}_{40}\text{Zr}_{2.5+x}\text{Cu}_{37.5-x}\text{Pd}_{7.5}\text{Sn}_5$ BMG in Hanks' solution. Pitting corrosion still occurs, however, and the E_{pit} value is 400 mV when $x=10$. Compared with this study, the Ti-based material with CNT does not exhibit pitting corrosion and has higher corrosion resistance.

The SEM micrographs of the surface of Ti-based BMG after potentiodynamic polarization show pitting corrosion and cavitation corrosion, as shown in Fig. 6. The microstructures of Ti-based BMG composites containing CNT display local pitting corrosion or crevice corrosion. We conjecture that the specimen surface had residue porosity, which cannot be completely eliminated during the consolidation step. The porosity is conducive to local pitting corrosion and crevice corrosion that occurs after potentiodynamic polarization. Therefore, pits of corrosion are distinct. Morrison et al. [15] and Hiromoto et al. [16] reported that the defects of the passive film on the specimen surface due to these inhom-

Table 1

Polarization results of $\text{Ti}_{50}\text{Cu}_{28}\text{Ni}_{15}\text{Sn}_7$ bulk metallic glasses containing CNT mixed for 8 h in Hanks' solution at 310 K.

	E_{corr} (V)	E_{pit} (V)	E_{pp} (V)	I_{corr} (A/cm^2)	$\eta_{\text{pit}}^{\text{a}}$ (V)	$\eta_{\text{pp}}^{\text{b}}$ (V)	CPR (mpy) ^c
Ti-based	-0.2735	0.2491	-0.0215	1.807×10^{-5}	0.5226	0.252	0.06347
CNT _{4%}	-0.2764	– ^d	– ^e	3.355×10^{-5}	– ^d	– ^e	0.10855
CNT _{8%}	-0.3286	– ^d	– ^e	2.395×10^{-5}	– ^d	– ^e	0.07287
CNT _{12%}	-0.2761	– ^d	– ^e	1.058×10^{-5}	– ^d	– ^e	0.03055

^a Pitting overpotential ($E_{\text{pit}} - E_{\text{corr}}$).

^b Protection overpotential ($E_{\text{pit}} - E_{\text{corr}}$).

^c Corrosion–penetration rate.

^d No pitting potential observed.

^e No protection potential observed.

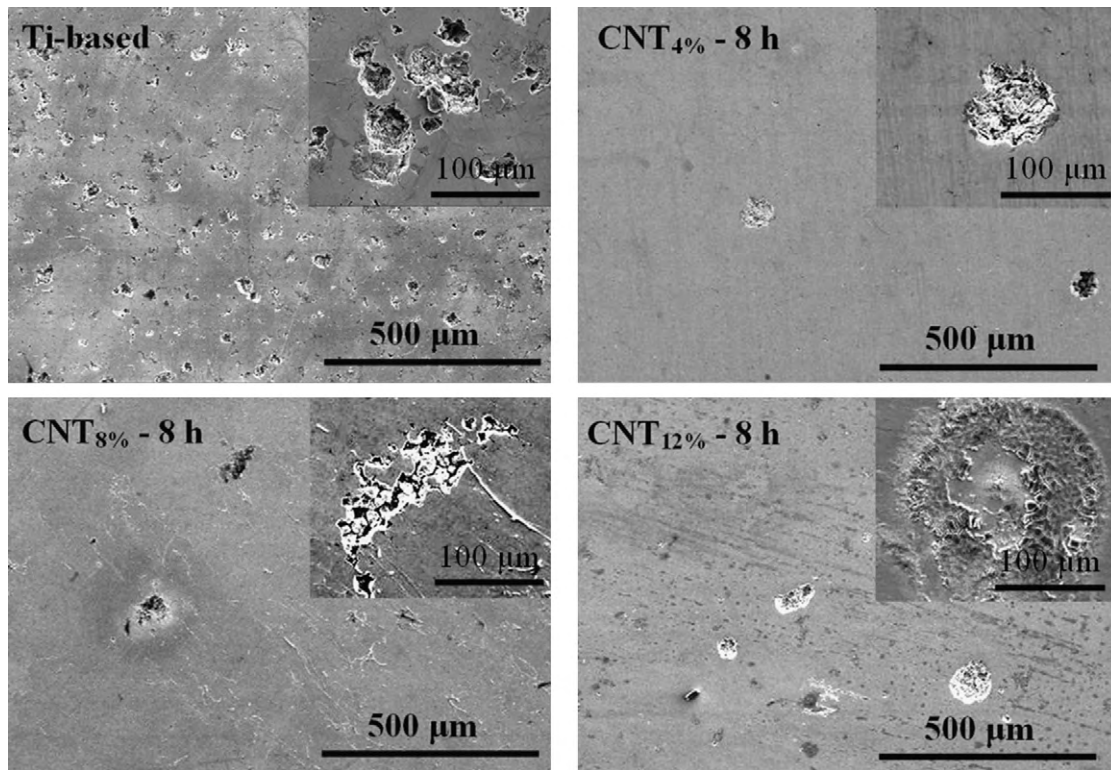


Fig. 6. SEM images of the $\text{Ti}_{50}\text{Cu}_{28}\text{Ni}_{15}\text{Sn}_7$ bulk metallic glasses containing CNT mixed for 8 h after corrosion testing.

genities serve as active sites for chloride ion attack and result in penetration of the passive film. The susceptibility to localized corrosion of BMG has been shown to increase with increasing concentrations of chloride ions in the Ti-based and Zr-based system. The further study by Qin et al. [17] explains that the Cu content of specimen surface is seriously decreased by chloride ion dissolution of the Cu, and there is higher heat of admixture in Ti with oxygen induce the passive film formed. Compared with this study, the Ti-based system immersed in Hanks' solution has similar results.

Though not shown here, XPS examination was used to reveal the surface films after corrosion tests. Ti-based bulk metallic glass and its 4% CNT-added composite exhibited TiO_2 and Cu_2O species. While CuCl_2 and CuSO_4 species were found on the surface of Ti-based BMG containing 12% CNT. This indicates that, though Ti-based BMG composites exhibited higher corrosion resistance than Ti-based BMG, the passive protective films, however, were different.

4. Conclusion

In the present study, amorphous $\text{Ti}_{50}\text{Cu}_{28}\text{Ni}_{15}\text{Sn}_7$ and its composite powders were successfully synthesized by the mechanical alloying of powder mixtures of pure Ti, Cu, Ni, Sn and CNT after 8 h milling. The metallic glass composite powders were found to exhibit a large supercooled liquid region before crystallization. The thermal stability of the amorphous matrix is affected by the presence of the CNT particles. Changes in T_g and T_x suggest that deviations in the chemical composition of the amorphous matrix developed due to a partial dissolution of the CNT species in the amorphous phase. BMG composite compact discs were obtained

by consolidating the 8 h as-milled composite powders by a vacuum hot pressing process. The results in Hanks' solution reveal that the Ti-based bulk metallic glass composites have high corrosion resistance and formed spontaneously passivated by anodic polarization with a passive current density of about 10^{-5} A/cm² in Hanks' solution. The higher corrosion resistance for the Ti-based bulk metallic glass composites was attributed to stable and protective passive films enriched with titanium and containing certain amounts of additional elements.

References

- [1] A. Inoue, *Acta Mater.* 48 (2000) 279–306.
- [2] A. Peker, W.L. Johnson, Beryllium bearing amorphous metallic alloys formed by low cooling rates, United States Patent No. 5, 288 (1994) 344.
- [3] H. Choi-Yim, W.L. Johnson, *Appl. Phys. Lett.* 71 (1997) 3808–3810.
- [4] C.P. Kim, R. Bush, A. Masuhr, H. Choi-Yim, W.L. Johnson, *Appl. Phys. Lett.* 79 (2001) 1456–1458.
- [5] C.C. Hays, C.P. Kim, W.L. Johnson, *Phys. Rev. Lett.* 84 (2000) 2901–2904.
- [6] A. Inoue, *Mater. Sci. Forum* 312–314 (1999) 307–314.
- [7] C.C. Wang, C.K. Lin, Y.L. Lin, J.S. Chen, R.R. Jen, P.Y. Lee, *Mater. Sci. Forum* 475–479 (2005) 3443–3450.
- [8] J. Eckert, M. Seidel, A. Kubler, U. Klement, L. Schultz, *Scripta Mater.* 38 (1998) 595–602.
- [9] W.H. Peter, R.A. Buchanan, C.T. Liu, P.K. Liaw, M.L. Morrison, J.A. Horton, C.A. Carmichael Jr., J.L. Wright, *Intermetallics* 10 (2002) 1157–1162.
- [10] F.X. Qin, M. Yoshimura, X.M. Wang, S.G. Zhu, A. Kawashima, K. Asami, A. Inoue, *Mater. Trans.* 48 (2007) 1855–1858.
- [11] C.K. Lin, S.S. Hong, P.Y. Lee, *Intermetallics* 8 (2000) 1043–1048.
- [12] F.R. de Boer, R. Boom, W.C.M. Mattens, A.R. Miedema, A.K. Niessen, *Cohesion in Metals Transition Metal Alloy*, 1988, pp. 723–729.
- [13] Z. Bian, M.X. Pan, Y. Zhang, W.H. Wang, *Appl. Phys. Lett.* 81 (2002) 4739–4741.
- [14] S. Deledda, J. Eckert, L. Schultz, *Mater. Sci. Forum* 360–362 (2001) 85–90.
- [15] M.L. Morrison, R.A. Buchanan, A. Peker, P.K. Liaw, J.A. Horton, *J. Non-Cryst. Solids* 353 (2007) 2115–2124.
- [16] S. Hiromoto, T. Hanawa, K. Ogawa, *Mater. Trans.* 44 (2003) 1824–1829.
- [17] C.L. Qin, J.J. Oak, N. Ohtsu, K. Asami, A. Inoue, *Acta Mater.* 55 (2007) 2057–2063.